

---

**Research Article**

## First-principles study of the adsorption behavior of Octyl- $\beta$ -D-xyloside surfactant on pristine Al<sub>12</sub>N<sub>12</sub> and B<sub>12</sub>N<sub>12</sub> nanocages

Hossein Khalafi<sup>1</sup>, Sara Ahmadi<sup>2\*</sup>

<sup>1</sup>Department of Chemistry, Fars Science and Research Branch, Islamic Azad University, Firoozabad, Iran

<sup>2</sup>Department of Chemistry, Firoozabad Branch, Islamic Azad University, Firoozabad, Iran

---

### ARTICLE INFO:

Received:  
4 July 2021

Accepted:  
18 August 2021

Available online:  
21 August 2021

✉: S. Ahmadi  
[saraah1380@gmail.com](mailto:saraah1380@gmail.com)

### ABSTRACT

The octyl- $\beta$ -D-xyloside is a biosurfactant with well-known roles in membrane protein systems. Using an efficient delivery system for these biosurfactants is of primary importance. This paper investigates the potential application of Al<sub>12</sub>N<sub>12</sub> and B<sub>12</sub>N<sub>12</sub> nanocages as an electronic sensor for octyl- $\beta$ -D-xyloside surfactant detection in the gas phase using density functional theory calculations. Our results show that the electronic properties of Al<sub>12</sub>N<sub>12</sub> and B<sub>12</sub>N<sub>12</sub> nanocages were significantly affected by the adsorption of the octyl- $\beta$ -D-xyloside molecule. The adsorption energies and enthalpies predicted a thermodynamically favorable chemisorption process. The AIM analysis reveals the formation of normal and bifurcated hydrogen bonds for Al<sub>12</sub>N<sub>12</sub> and B<sub>12</sub>N<sub>12</sub> nanocages whilst, for O

3, O2, and O4 positions we identify the inter/intra-molecular hydrogen bonds. The NBO results revealed a charge transfer from the adsorbed octyl- $\beta$ -D-xyloside molecule to the nanocluster. Our finding revealed although both Al<sub>12</sub>N<sub>12</sub> and B<sub>12</sub>N<sub>12</sub> nanocages have the ability to detect and adsorb the octyl- $\beta$ -D-xyloside but, the adsorption over the Al<sub>12</sub>N<sub>12</sub> is not favorable due to the high recovery time. Whilst, the adsorption of the octyl- $\beta$ -D-xyloside through O3 with less steric factor on the B<sub>12</sub>N<sub>12</sub> nanocage and the recovery time of  $8.14 \times 10^{-3}$  S, is the best adsorption site.

**Keywords:** DFT, Octyl- $\beta$ -D-xyloside, Al<sub>12</sub>N<sub>12</sub>, B<sub>12</sub>N<sub>12</sub>, Nanocage, Adsorption, sensor.

---

## 1. Introduction

Biosurfactants (BS) are a valuable group of bio related compounds, classified principally according to their nature and chemical composition [1, 2]. Synthesis from renewable sources, low toxicity, the capacity to refract or detriment the cell membrane, and excellent biological activity which are essential for therapeutic and biomedical can be motivated to enhancement their importance in the medical, pharmaceutical, and therapeutic. They can be used as antimicrobial agents to conduct cellular analysis by enhancing the penetration of the membrane, and metabolite stream [3-5]. *Lactococcus lactis* is a probiotic bacteria that play a number of potential roles in human health by producing a variety of secondary metabolites [6, 7]. One of the main secondary metabolites generated by *Lactococcus lactis* is xylolipid which prohibits the formation of the pathogenic microbial population in the human bowel by decomposition of the cell wall.

The octyl- $\beta$ -D-xyloside is a biosurfactant that belongs to the glycolipid families (Fig. 1). This monosaccharide is a significant component of the pentose fraction in hemicellulose [8], consists of a water-loving hydrophilic sugar head group, and water-hating hydrophobic alkyl chain and generates a substrate for the manufacture of xylitol, as a food additive, sugar substitute, and also to advance better dental health and anticavity agents [9]. Accordingly, using an efficient delivery system for these biosurfactants is of primary importance. Recently, nanostructures like nanowires, nanotubes, and nanocages have been paid to great consideration as drug delivery systems [10-16]. Nanoparticles with slender size and surface ligand modification are attractive candidates for transducers of biorecognition binding and molecular structure [17, 18]. The remarkably high extinction coefficients of nanoclusters make them appropriate for optical signal transducers of molecular binding in comparison to any organic and inorganic chromophores. These aspects parallel with the toxicity of carbon compounds, encourage scientists to consider the efficiency of the inorganic nanomaterials.

Drug delivery systems made up of nanoparticles can significantly improve the drug treatment to the patient tissue as well as reducing the adverse effects of drugs on the healthy tissues [19, 20]. The incorporation of chemotherapeutic drugs and receptors specific for the target cells into nanocarriers is a promising strategy in the drug delivery area [21].

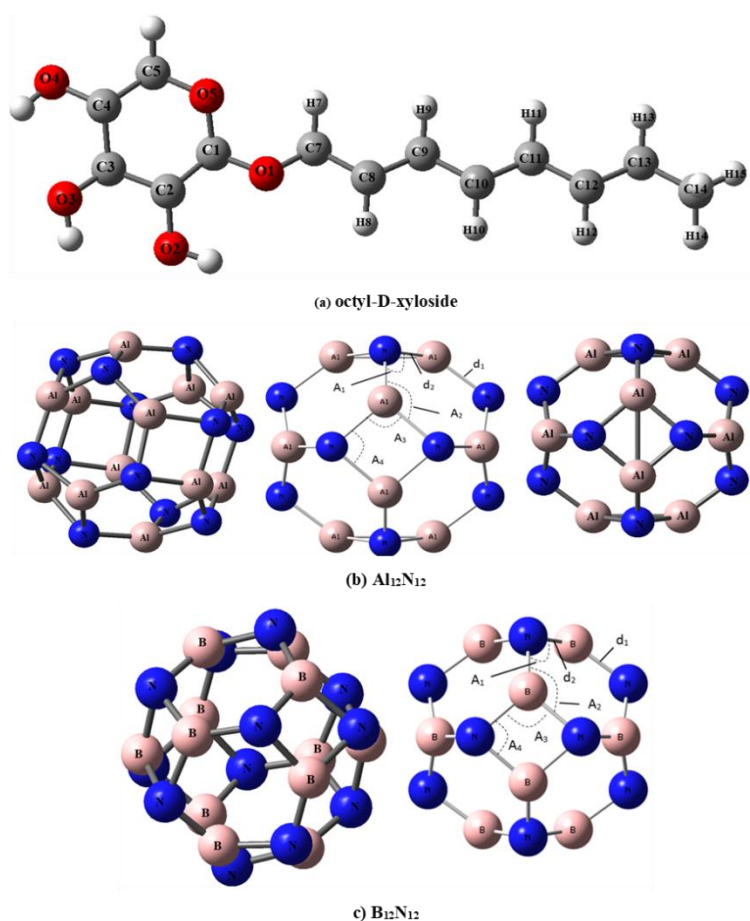


**Fig. 1** The scheme of (a) octyl- $\beta$ -D-xyloside (the numbering of the sugar ring is according to IUPAC nomenclature of glycolipids and indicates possible absorption positions of different oxygen on the nanocluster), (b)  $\text{Al}_{12}\text{N}_{12}$ , and (c)  $\text{B}_{12}\text{N}_{12}$  nanocages optimized at the B3LYP/6-311++G\*\* level of theory.

The combination of the atoms of groups III and V in the periodic table are good candidates to use as the nanostructure compound. Among different nanostructures,  $\text{Al}_{12}\text{N}_{12}$  and  $\text{B}_{12}\text{N}_{12}$  nanocages have mainly engrossed scientists' attention owing to their low electron affinity, large band gap, special sensing, and superior physical and chemical properties [22-26]. It seems that the  $sp^2$  hybridization of metal–nitrogen bonds can be considered as the energetic

stability reason of  $Al_{12}N_{12}$  nanocage [27]. In this research, we investigate the adsorption behavior, electronic, and reactivity of octyl- $\beta$ -D-xyloside toward the  $Al_{12}N_{12}$  and  $B_{12}N_{12}$  nanocages with the aim of using these nanocages as the delivery system for octyl- $\beta$ -D-xyloside to the cell membrane.

## 2. Methodology

The initial structure of  $Al_{12}N_{12}$ ,  $B_{12}N_{12}$ , and octyl- $\beta$ -D-xyloside were modeled using Gauss View 5.0 [22] and geometrically optimized within the framework of density functional theory at the B3LYP/6-31G level of theory (Fig.1). Subsequently, all five orientations of octyl- $\beta$ -D-xyloside (O1, O2, O3, O4, and O5) as a ligand, were considered to approach  $Al_{12}N_{12}$  and  $B_{12}N_{12}$  nanocages (Fig. 2). Finally, the considered complexes (octyl- $\beta$ -D-xyloside and nanocage) were geometrically optimized at the B3LYP/ 6-311++G\*\* using the Gaussian 09 computational package [23] in the gas phase. The hybrid B3LYP functional provides an efficient and robust basis in nanostructure studies [24-26]. Normal mode frequency analysis was performed numerically and examine the nature of the stationary points founded in the potential energy surfaces (PES). All optimized structures in the PES were real minimum stationary points due to the absence of negative frequency in normal analyses. The adsorption energies of the studied complexes are corrected separately, for both zero point energy (ZPE) and basis set superposition error (BSSE) using the counterpoise correction scheme outlined by Boys and Bernardi [28]. The adsorption energy ( $E_{ads}$ ) of octyl- $\beta$ -D -xyloside over the surface of pristine  $Al_{12}N_{12}$  and  $B_{12}N_{12}$  nanocages is defined as:

$$E_{ad} = E(\text{complex}) - [E(Al_{12}N_{12} \text{ or } B_{12}N_{12}) + E(\text{octyl} - \beta - D - \text{xyloside})] \quad (1)$$

Where  $E$  (complex) is the total energy of the adsorbed octyl- $\beta$ -D-xyloside on the surface of the  $Al_{12}N_{12}$  or  $B_{12}N_{12}$  nanocages,  $E$  ( $Al_{12}N_{12}$  or  $B_{12}N_{12}$ ) and  $E$  (octyl- $\beta$ -D-xyloside) are the

energies of the  $\text{Al}_{12}\text{N}_{12}$ ,  $\text{B}_{12}\text{N}_{12}$ , and octyl- $\beta$ -D-xyloside respectively. The Atoms in Molecules (AIM) analyses were carried out using the AIM2000 package [27] to analyze the electron density and bonding characteristics of the investigated complexes. The electronic density of states (DOS) was plotted using Gauss Sum [28].

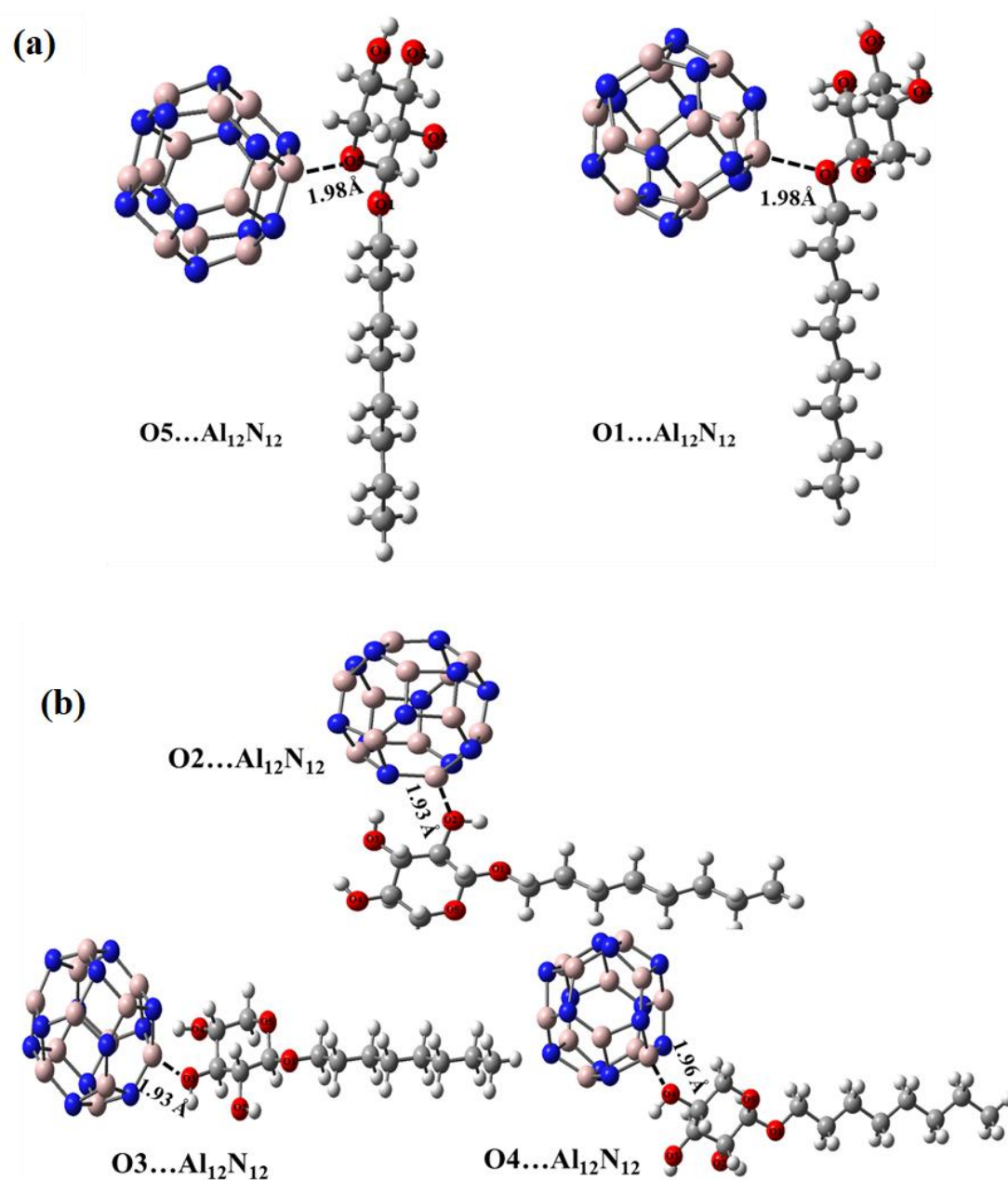


**Fig. 2** (a) The optimized structures of adsorbed octyl- $\beta$ -D-xyloside on the pristine  $\text{Al}_{12}\text{N}_{12}$  from O1 and O5 positions (b) from O2, O3, and O4 positions at the B3LYP/6-311++G\*\* level of theory in the gas phase.

### 3. Results and discussion

#### 3.1 Geometry optimization and validation

The optimized geometries of pristine  $\text{Al}_{12}\text{N}_{12}$  and  $\text{B}_{12}\text{N}_{12}$  nanocages show the four and six-membered rings of each nanocage are not completely planar [29]. The average bond lengths and bond angles for Al–N and B–N in four and six-membered rings (see Fig.1-b and 1-c, for labeling) are tabulated in Table 1. The average bond lengths in the six-membered ring for Al–N and B–N are 1.79 and 1.43 Å, respectively, while it is 1.85 and 1.48 Å in the four-membered ring. The average bond lengths ( $d_1$  and  $d_2$ ) of  $\text{Al}_{12}\text{N}_{12}$  nanocage are longer than that of  $\text{B}_{12}\text{N}_{12}$  in both six and four-membered rings. However, the bond lengths of the six-membered ring in  $\text{Al}_{12}\text{N}_{12}$  and  $\text{B}_{12}\text{N}_{12}$  nanocages are shorter than the four-membered rings. The bond angles for N–Al–N in  $\text{Al}_{12}\text{N}_{12}$  nanocage are,  $A_2=125.70^\circ$  and  $A_3=94.50^\circ$  and for Al–N–Al are,  $A_1=112.50^\circ$  and  $A_4=84.40^\circ$ , in six and four-membered rings respectively. Whilst, in the  $\text{B}_{12}\text{N}_{12}$  nanocage, the N–B–N angle has the values of  $A_2=125.70^\circ$  and  $A_3=98.10^\circ$  and the B–N–B angle has the values of  $A_1=111.10^\circ$  and  $A_4=80.50^\circ$ , in six and four-membered rings respectively, which are very close in both nanocages.

It is clear that the bond angles of N–Al–N and N–B–N are larger than the bond angles of Al–N–Al and B–N–B in both six and four-membered rings. This could be related to the pressure caused by the non-bonded electrons of the nitrogen atom. It is notable that, the bond angles in six-membered rings ( $A_1$  and  $A_2$ ) are almost equal for  $\text{Al}_{12}\text{N}_{12}$  and  $\text{B}_{12}\text{N}_{12}$  nanocages whilst, in four-membered rings ( $A_3$  and  $A_4$ ) they have different values. In 6-membered rings with a little wrinkled shape, the difference between the angles of  $\text{Al}_{12}\text{N}_{12}$  and  $\text{B}_{12}\text{N}_{12}$  are small, but in 4-membered rings, the angling pressure does not let wrinkle and the four-membered ring is almost flat. This lead to a greater difference between the angles of  $\text{Al}_{12}\text{N}_{12}$

and  $B_{12}N_{12}$  in the four-membered rings. The same results were observed for  $A_3$  and  $A_4$  of both nanocages. These results are in line with other literature [20].

**Table 1.** Selected bond lengths ( $d_1$  and  $d_2$ ) (in Å) and bond angles  $A_1$ ,  $A_2$ ,  $A_3$ , and  $A_4$  (in °) for  $Al_{12}N_{12}$  and  $B_{12}N_{12}$  nanocages in the gas phase. Labeling is according to Fig. 1-b, and 1-c.

Properties	Ring	$Al_{12}N_{12}$	$B_{12}N_{12}$
$d_1$	6	1.79	1.43
$d_2$	4	1.85	1.48
$A_1=Al-N-Al/B-N-B$	6	112.50	111.10
$A_2=N-Al-N/N-B-N$	6	125.70	125.70
$A_3=N-Al-N/N-B-N$	4	94.50	98.10
$A_4=Al-N-Al/B-N-B$	4	84.40	80.50

To specify the orientations for octyl- $\beta$ -D-xyloside adsorption over the  $Al_{12}N_{12}$  and  $B_{12}N_{12}$  nanocages, we placed the octyl- $\beta$ -D-xyloside molecule through different oxygen atoms (O1, O2, O3, O4, and O5) at a reasonable distance from the pristine  $Al_{12}N_{12}$  and  $B_{12}N_{12}$  nanocage surfaces and let the system optimize for finding the most stable configuration in the gas phase (Fig. 2 and Fig. 3). The oxygen atoms in the octyl- $\beta$ -D-xyloside molecule divided into two categories; i: O2, O3, and O4 which connected to the hydrogen and represent hydroxyl groups (HO<sub>2</sub>, HO<sub>3</sub>, and HO<sub>4</sub>); ii: O1 and O5 which connected only to carbons.

The calculated values of the adsorption energies along with the values of charge transfer based on natural bond orbital analysis (NBO), as well as the equilibrium distance of each oxygen atom of octyl- $\beta$ -D-xyloside to the nanocages are listed in Table 2. Table 2 shows, the adsorption energies trend for  $Al_{12}N_{12}$  is  $O1 > O5$  and  $O3 > O2 > O4$  for two types of oxygen atoms. The negative values of the adsorption energies indicate the chemisorption process. The O3 position with the adsorption energies of -155.09 kJ/mol, is the most stable adsorption position. This could be due to the less spatial repulsion around the O3 position, which has an

equatorial direction as the alkyl chain. On the other hand, the bond distance trend between the  $\text{Al}_{12}\text{N}_{12}$  nanocage and hydroxyl groups of octyl- $\beta$ -D-xyloside is  $\text{O}_4 > \text{O}_2 > \text{O}_3$ . As it turns out, the adsorption energy is inversely related to the bond length. Accordingly, the  $\text{O}_3$  position with the most stable adsorption energy has the least bond length of 1.93 Å. The formed bond distances from the  $\text{O}_1$  and  $\text{O}_5$  positions are equal (1.98 Å) in  $\text{Al}_{12}\text{N}_{12}$ . However, the less steric factor of the sugar ring around the  $\text{O}_1$  position causes more stability for  $\text{O}_1$ — $\text{Al}_{12}\text{N}_{12}$  complex than  $\text{O}_5$ — $\text{Al}_{12}\text{N}_{12}$ .

**Table 2.** The calculated adsorption energies ( $E_{ad}$ ) in kJ/mol, equilibrium adsorbed distance ( $d$ ) in (Å), and the values of charge transfer  $q_{NBO}$  ( $e$ ) at the B3LYP/6-311++G\*\* level of theory with BSSE superposition error correction in the gas phase.

Oxygen type	Complex	$E_{ad}$	$d(\text{nanocage—O}_n)$	$q_{NBO}$
O1, O5	$\text{O}_1$ — $\text{Al}_{12}\text{N}_{12}$	-133.62	1.98	-0.072
	$\text{O}_5$ — $\text{Al}_{12}\text{N}_{12}$	-116.25	1.98	-0.090
O3, O2, O4	$\text{O}_3$ — $\text{Al}_{12}\text{N}_{12}$	-155.09	1.93	-0.057
(hydroxyl groups)	$\text{O}_2$ — $\text{Al}_{12}\text{N}_{12}$	-154.91	1.95	-0.055
	$\text{O}_4$ — $\text{Al}_{12}\text{N}_{12}$	-121.31	1.97	-0.058
O5, O1	$\text{O}_5$ — $\text{B}_{12}\text{N}_{12}$	-55.14	1.65	-0.094
	$\text{O}_1$ — $\text{B}_{12}\text{N}_{12}$	-50.96	1.66	-0.075
O3, O2, O4	$\text{O}_3$ — $\text{B}_{12}\text{N}_{12}$	-82.08	1.62	-0.060
(hydroxyl groups)	$\text{O}_2$ — $\text{B}_{12}\text{N}_{12}$	-80.61	1.64	-0.059
	$\text{O}_4$ — $\text{B}_{12}\text{N}_{12}$	-64.76	1.64	-0.059

The adsorption energy trend for  $\text{B}_{12}\text{N}_{12}$  in the gas phase is  $\text{O}_5 > \text{O}_1$  and  $\text{O}_3 > \text{O}_2 > \text{O}_4$ . Hence,  $\text{O}_5$ — $\text{B}_{12}\text{N}_{12}$  complex is more stable than  $\text{O}_1$ — $\text{B}_{12}\text{N}_{12}$  complex.

As such, the  $O_3-B_{12}N_{12}$  with the least spatial hinder and highest adsorption energy of -82.08 kJ/mol is the most stable complex among  $O_3-B_{12}N_{12}$ ,  $O_2-B_{12}N_{12}$ , and  $O_4-B_{12}N_{12}$  complexes. This indicates the adsorption over the O3 position is more favorable. The O1 and O5 oxygen atoms (without hydrogen donor) form a weaker bond which can be interpreted by the NBO analysis.

The NBO results represent the net charge transfer during the adsorption of octyl- $\beta$ -D-xyloside on the surface of pristine  $Al_{12}N_{12}$  and  $B_{12}N_{12}$  nanocages. Table 2 shows the O1 and O5 oxygen atoms with free electron pairs have the ability to form a dative bond with the empty orbital of the aluminum and boron atoms in each nanocage. As a result, a charge transfer from oxygen atom to aluminum and boron atoms will happen. This charge transfer resulted in a reduction of the negative charge of oxygen, which compensates by adsorbing electrons from neighboring carbon and hydrogen atoms. In fact, the negative NBO charge values are a witness to show a partial charge transfer from the attached carbon and hydrogen atoms after bonding.

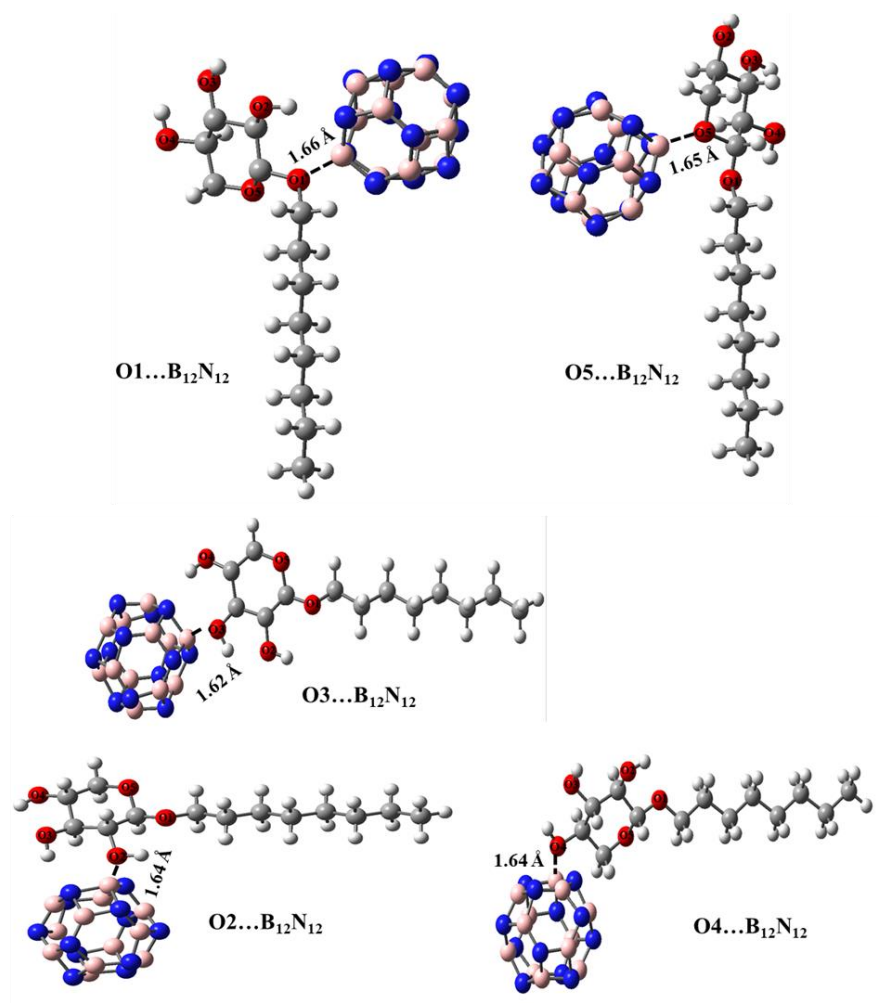


**Fig. 3** (a) The optimized structures of adsorbed octyl- $\beta$ -D-xyloside on the pristine B<sub>12</sub>N<sub>12</sub> nanocage from O1 and O5 positions (b) from O2, O3, and O4 positions at the B3LYP/6-311++G\*\* level of theory in the gas phase.

### 3.2 Electronic properties

In order to understand the changes of the electronic properties of Al<sub>12</sub>N<sub>12</sub> and B<sub>12</sub>N<sub>12</sub> nanocages after the complexation with octyl- $\beta$ -D-xyloside, we depicted the frontier molecular orbitals (highest occupied molecular orbital (HOMO) and lowest unoccupied molecular orbital (LUMO)) Fig.4, as well as the density of states (DOSs) (Fig. 4 and SF1), for pristine Al<sub>12</sub>N<sub>12</sub> and B<sub>12</sub>N<sub>12</sub> nanocages and their complexes with octyl- $\beta$ -D-xyloside from different oxygen atoms.

According to Table 3, upon the interaction with octyl- $\beta$ -D-xyloside, notable changes were observed in the HOMO and LUMO energies of  $\text{Al}_{12}\text{N}_{12}$  nanocage such that, the energies of HOMO and LUMO in  $\text{O}_n\text{—Al}_{12}\text{N}_{12}$  and  $\text{O}_n\text{—B}_{12}\text{N}_{12}$  complexes were increased whilst, the band gaps decreased. The most changes in the band gap were observed for  $\text{O}_5\text{—Al}_{12}\text{N}_{12}$  complex and the band gap decreased from 3.894 to 3.579 eV. In addition, for the  $\text{B}_{12}\text{N}_{12}$  nanocage, the band gap also decreased from 6.774 to 6.641 eV for  $\text{O}_1\text{—B}_{12}\text{N}_{12}$  during the complexation with octyl- $\beta$ -D-xyloside. It is important to note that in comparison between the adsorption from O1 and O5, the O1 in  $\text{Al}_{12}\text{N}_{12}$  and O5 in  $\text{B}_{12}\text{N}_{12}$  nanocage, have the most energy gaps.

**Table 3.** The energies of  $E_{\text{HOMO}}$ ,  $E_{\text{LUMO}}$ , and  $E_{\text{gap}}$ , (all in eV) for  $\text{Al}_{12}\text{N}_{12}$  and  $\text{B}_{12}\text{N}_{12}$  and their complexes with octyl- $\beta$ -D-xyloside through different oxygens.

Oxygen type	Complex	$E_{\text{HOMO}}$ (eV)	$E_{\text{LUMO}}$ (eV)	$E_{\text{gap}}$ (eV)	$\% \Delta E^\circ$
	$\text{Al}_{12}\text{N}_{12}$	-6.416	-2.522	3.894	-
O1, O5	$\text{O}_1\text{—Al}_{12}\text{N}_{12}$	-6.047	-2.224	3.823	-1.823
	$\text{O}_5\text{—Al}_{12}\text{N}_{12}$	-5.906	-2.327	3.579	-8.084
O3, O2, O4 (hydroxyl groups)	$\text{O}_3\text{—Al}_{12}\text{N}_{12}$	-6.033	-2.158	3.875	-0.480
	$\text{O}_2\text{—Al}_{12}\text{N}_{12}$	-6.048	-2.201	3.847	-1.202
	$\text{O}_4\text{—Al}_{12}\text{N}_{12}$	-5.961	-2.101	3.859	-0.896
	$\text{B}_{12}\text{N}_{12}$	-7.634	-0.860	6.774	-
O5, O1	$\text{O}_5\text{—B}_{12}\text{N}_{12}$	-6.780	-0.107	6.673	-1.497
	$\text{O}_1\text{—B}_{12}\text{N}_{12}$	-6.945	-0.303	6.641	-1.959
O3, O2, O4 (hydroxyl groups)	$\text{O}_3\text{—B}_{12}\text{N}_{12}$	-6.883	-0.157	6.726	-0.709
	$\text{O}_2\text{—B}_{12}\text{N}_{12}$	-7.031	-0.326	6.705	-1.014
	$\text{O}_4\text{—B}_{12}\text{N}_{12}$	-6.780	-0.116	6.682	-1.354

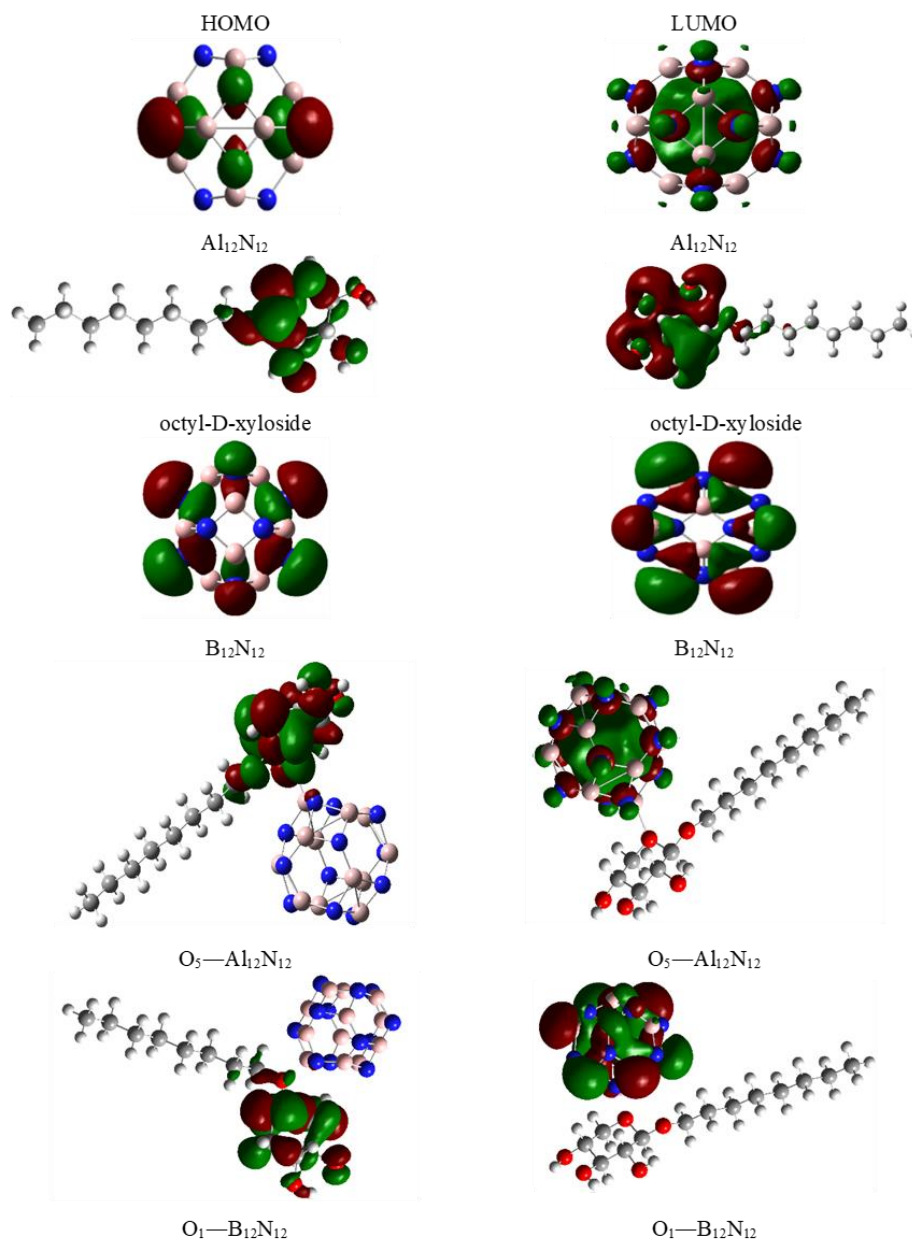


**Fig. 4** The HOMO and LUMO distribution for  $\text{Al}_{12}\text{N}_{12}$ , octyl- $\beta$ -D-xyloside, and  $\text{B}_{12}\text{N}_{12}$  and  $\text{O}_5\text{—Al}_{12}\text{N}_{12}$  and  $\text{O}_1\text{—B}_{12}\text{N}_{12}$  complexes in the gas phase at the B3LYP/6-311++G\*\* level of theory

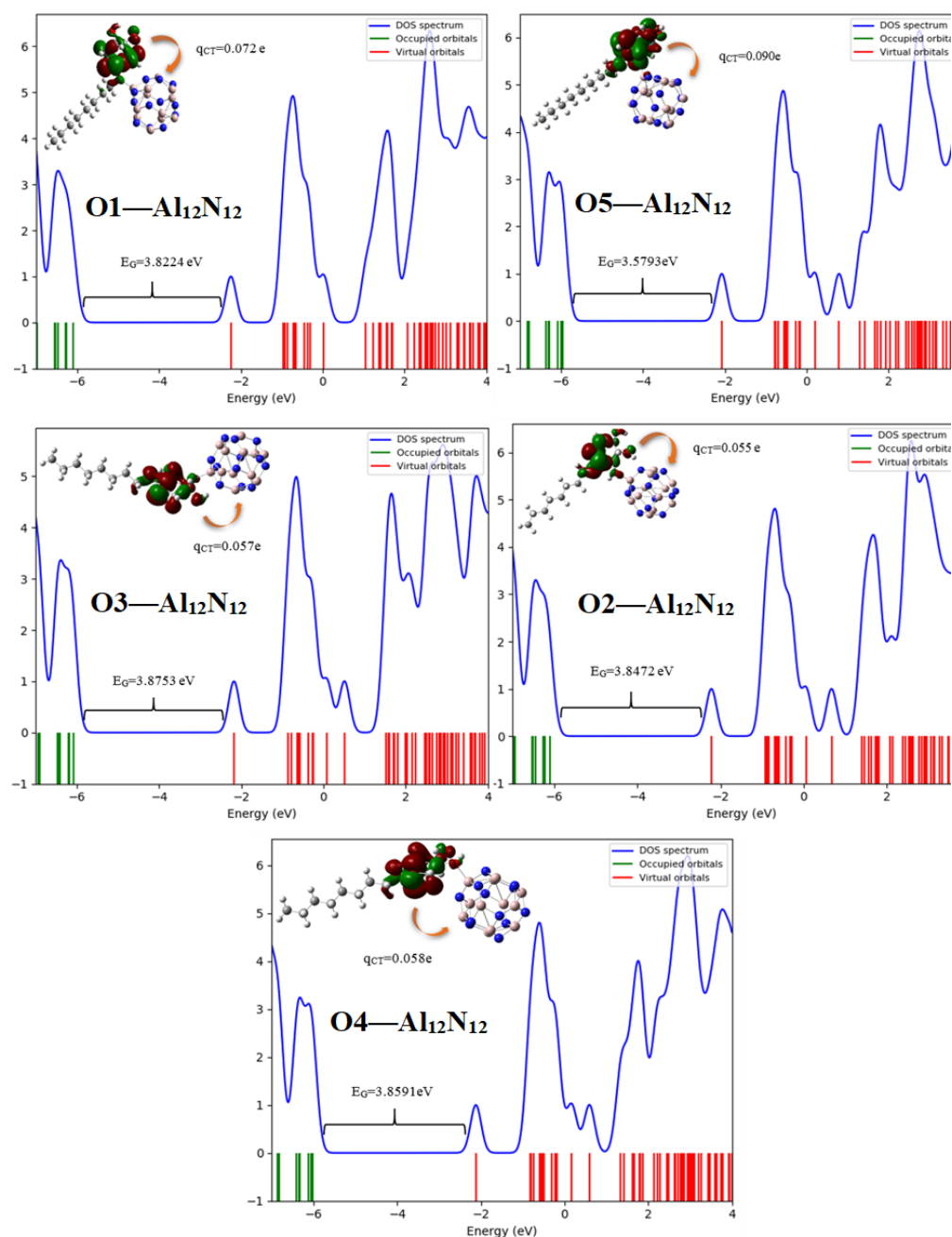


**Fig. 5** Density of states for the complexation of  $\text{Al}_{12}\text{N}_{12}$  with octyl- $\beta$ -D-xyloside from different oxygen atoms at the B3LYP/6-311++G\*\* level of theory in the gas phase.

### 3.3 Atoms in Molecules analysis

Atoms in molecules (AIM) theory [30] is a powerful tool of modern quantum chemistry to analyze bond types at different interaction sites of a system via different key concepts such as electron density  $\rho(r)$ , and the Laplacian of the electron density,  $\nabla^2\rho(r)$ , which is the sum of

the curvature in the charge density along any orthogonal coordinate axes computed at the bond critical point (BCP), as well as kinetic energy density ( $G$ ), potential energy ( $V$ ) and total energy ( $H$ ) [31]. The sign of Laplacian of the electron density,  $\nabla^2\rho(r)$ , at the BCP indicates charge density is concentrated for  $\nabla^2\rho(r) < 0$  as the covalent bond, while  $\nabla^2\rho(r) > 0$  show a depleted charge density, as in closed shell (electrostatic) interactions. It should be mentioned that H-bond is characterized by  $\nabla^2\rho(r) < 0$ ,  $H(r) < 0$  for strong H-bond, while medium H-bond (partially covalent-partially electrostatic) with  $\nabla^2\rho(r) > 0$ ,  $H(r) < 0$ , and  $\nabla^2\rho(r) > 0$ ,  $H(r) > 0$  are established for weak H-bond [30]. The positive values of the Laplacian indicate a depletion in charge density as in closed shell (electrostatic) interactions. Jeffrey and Saenger [32, 33] defined the hydrogen bond with the terms of normal (two-center), bifurcated (three-center), and trifurcated (four-center) hydrogen bond (see Fig. 6). The existence of bifurcated H-bond in different complexes was investigated computationally recently [34-37].

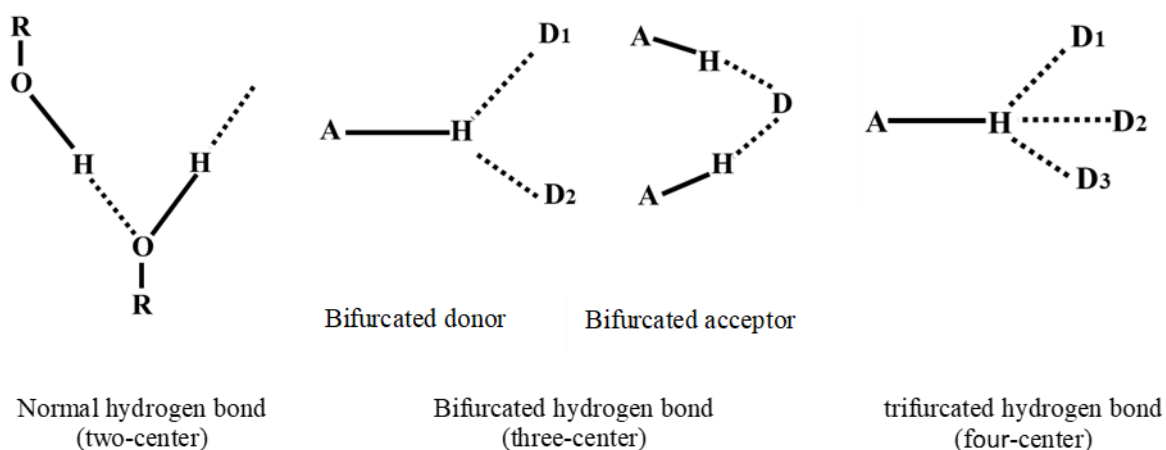


**Fig. 6** Three different types of hydrogen bond according to Jeffrey and Saenger [32,33]

**Table 4.** Equilibrium distance ( $d$ ) (in Å) and topological parameters (all in a.u) for adsorption of the octyl- $\beta$ -D-xyloside on the pristine Al<sub>12</sub>N<sub>12</sub> nanocage from different oxygen atoms (O1, O2, O3, O4, and O5) at the B3LYP/6-311++G\*\* level of theory in the gas phase.

Oxygen type	Complexes	Bonds	$d$	$\rho(r)$	$\nabla^2\rho(r)$	$G_{(r)}$	$V_{(r)}$	$H_{(r)}$
i: O1	O <sub>1</sub> —Al <sub>12</sub> N <sub>12</sub>	<b>O<sub>1</sub>...Al</b>	1.98	0.0474	0.2923	0.0689	-0.0648	0.0041
		O <sub>2</sub> -HO <sub>2</sub> ...N <sub>1</sub>	1.77	0.0450	0.1142	0.0322	-0.0359	-0.0037
		C <sub>7</sub> -H <sub>7</sub> ...N <sub>2</sub>	2.53	0.0121	0.0387	0.0086	-0.0075	0.0011
i: O5	O <sub>5</sub> —Al <sub>12</sub> N <sub>12</sub>	<b>O<sub>5</sub>...Al</b>	1.98	0.0477	0.2959	0.0697	-0.0655	0.0042
		C <sub>7</sub> -H <sub>7</sub> ...N <sub>1</sub>	2.64	0.0093	0.0273	0.0060	-0.0053	0.0008
		C <sub>5</sub> -H <sub>5</sub> ...N <sub>2</sub>	2.52	0.0121	0.0385	0.0086	-0.0075	0.0011
		C <sub>8</sub> -H <sub>8</sub> ...N <sub>1</sub>	3.62	0.0022	0.0061	0.0011	-0.0007	0.0004
		C <sub>2</sub> -H <sub>2</sub> ...N <sub>3</sub>	2.71	0.0084	0.0245	0.0053	-0.0046	0.0008
ii: O3 (hydroxyl groups)	O <sub>3</sub> —Al <sub>12</sub> N <sub>12</sub>	<b>O<sub>3</sub>...Al</b>	1.93	0.0508	0.3506	0.0803	-0.0730	0.0073
		O <sub>4</sub> -HO <sub>4</sub> ...N <sub>1</sub>	1.82	0.0405	0.1035	0.0029	-0.0317	-0.0288
ii: O2 (hydroxyl groups)	O <sub>2</sub> —Al <sub>12</sub> N <sub>12</sub>	<b>O<sub>2</sub>...Al</b>	1.95	0.0497	0.3321	0.0766	-0.0701	0.0065
		O <sub>3</sub> -HO <sub>3</sub> ...N <sub>1</sub>	1.77	0.0452	0.1150	0.0037	-0.0361	-0.0324
		O <sub>2</sub> -HO <sub>2</sub> ...O <sub>1</sub>	2.14	0.0195	0.0772	0.0184	-0.0175	0.0009
ii: O4 (hydroxyl groups)	O <sub>4</sub> —Al <sub>12</sub> N <sub>12</sub>	<b>O<sub>4</sub>...Al</b>	1.97	0.0488	0.3124	0.0731	-0.0681	0.0050
		C <sub>3</sub> -H <sub>3</sub> ...N <sub>1</sub>	2.84	0.0067	0.0202	0.0042	-0.0034	0.0008
		C <sub>5</sub> -H <sub>5</sub> ...N <sub>1</sub>	2.74	0.0081	0.0241	0.0052	-0.0043	0.0009

**Table 5.** Equilibrium distance ( $d$ ) (in Å) and topological parameters (all in a.u) for adsorption of the octyl- $\beta$ -D-xyloside on the pristine B<sub>12</sub>N<sub>12</sub> nanocage from different oxygen atoms (O1, O2, O3, O4, and O5) at the B3LYP/6-311++G\*\* level of theory in the gas phase.

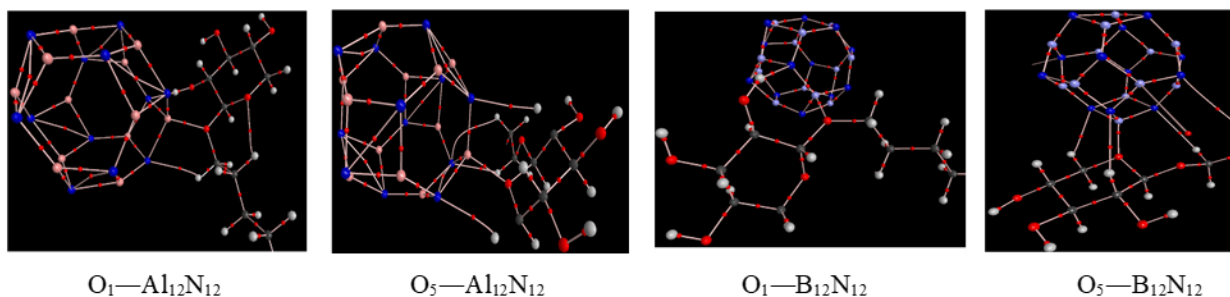
Oxygen type	Complexes	Bonds	$d$	$\rho(r)$	$\nabla^2\rho(r)$	$G_{(r)}$	$V_{(r)}$	$H_{(r)}$
i: O5	O <sub>5</sub> —B <sub>12</sub> N <sub>12</sub>	<b>O<sub>5</sub>...B</b>	1.66	0.0904	0.2560	0.1203	-0.1766	-0.0563
		C <sub>7</sub> -H <sub>7</sub> ...N <sub>1</sub>	2.55	0.0104	0.0318	0.0071	-0.0062	0.0009
		C <sub>8</sub> -H <sub>8</sub> ...N <sub>2</sub>	3.15	0.0032	0.0107	0.0020	-0.0013	0.0007
		C <sub>5</sub> -H <sub>5</sub> ...N <sub>3</sub>	2.34	0.0159	0.0574	0.0125	-0.0107	0.0018
		C <sub>2</sub> -H <sub>2</sub> ...N <sub>4</sub>	2.55	0.0106	0.0321	0.0071	-0.0062	0.0009
i: O1	O <sub>1</sub> —B <sub>12</sub> N <sub>12</sub>	<b>O<sub>1</sub>...B</b>	1.66	0.0900	0.2608	0.1208	-0.1765	-0.0556
		O <sub>2</sub> -HO <sub>2</sub> ...N <sub>1</sub>	1.97	0.0291	0.0803	0.0211	-0.0222	-0.0011
ii: O3 (hydroxyl groups)	O <sub>3</sub> —B <sub>12</sub> N <sub>12</sub>	<b>O<sub>3</sub>...B</b>	1.64	0.0973	0.3132	0.1376	-0.1968	-0.0593
		O <sub>4</sub> -HO <sub>4</sub> ...N <sub>1</sub>	1.96	0.0292	0.0825	0.0215	-0.0225	-0.0009
		O <sub>3</sub> -HO <sub>3</sub> ...O <sub>2</sub>	2.09	0.0203	0.0793	0.0192	-0.0185	0.0007
ii: O4 (hydroxyl groups)	O <sub>4</sub> —B <sub>12</sub> N <sub>12</sub>	<b>O<sub>4</sub>...B</b>	1.64	0.0944	0.3124	0.1346	-0.1912	-0.0565
		O <sub>4</sub> -HO <sub>4</sub> ...O <sub>3</sub>	2.18	0.0175	0.0741	0.0173	-0.0160	0.0013
		C <sub>3</sub> -H <sub>3</sub> ...N <sub>1</sub>	2.66	0.0088	0.0265	0.0058	-0.0050	0.0008
		C <sub>5</sub> -H <sub>5</sub> ...N <sub>1</sub>	3.90	0.0066	0.0234	0.0048	-0.0037	0.0011
ii: O2 (hydroxyl groups)	O <sub>2</sub> —B <sub>12</sub> N <sub>12</sub>	<b>O<sub>2</sub>...B</b>	1.62	0.0986	0.3366	0.1432	-0.2021	-0.0590
		C <sub>1</sub> -H <sub>1</sub> ...N <sub>1</sub>	2.79	0.0069	0.0214	0.0045	-0.0037	0.0008
		O <sub>3</sub> -HO <sub>3</sub> ...N <sub>2</sub>	2.01	0.0268	0.0743	0.0193	-0.0201	-0.0008
		O <sub>2</sub> -HO <sub>2</sub> ...O <sub>1</sub>	2.18	0.0180	0.0749	0.0175	-0.0162	0.0013

According to Tables 4-5 and Fig. 7; complexes with oxygen type (i) such as  $O_1-Al_{12}N_{12}$ ,  $O_5-Al_{12}N_{12}$ ,  $O_1-B_{12}N_{12}$ , and  $O_5-B_{12}N_{12}$  illustrate only intermolecular hydrogen bond whereas complexes with oxygen type (ii) such as  $O_3-Al_{12}N_{12}$ ,  $O_2-Al_{12}N_{12}$ ,  $O_4-Al_{12}N_{12}$ ,  $O_3-B_{12}N_{12}$ ,  $O_4-B_{12}N_{12}$ , and  $O_2-B_{12}N_{12}$  can form the inter/intra molecular hydrogen bond. The lack of hydrogen on the  $O_1$  and  $O_5$  causes to behave only as an acceptor, whilst,  $O_2$ ,  $O_3$ , and  $O_4$  can act as donor and acceptor. On the other hand, during the complexation through  $O_5$  and  $O_4$  in  $Al_{12}N_{12}$  we can see the formation of the bifurcated hydrogen bond of  $C_7-H_7...N_1$  and  $C_8-H_8...N_1$  in  $O_5-Al_{12}N_{12}$  and  $C_3-H_3...N_1$  and  $C_5-H_5...N_1$  in  $O_4-Al_{12}N_{12}$ . This indicates the  $N_1$  atom involves into three different bonds simultaneously in each complex. In addition, in the  $B_{12}N_{12}$  complex, the only complexation through  $O_4$  can form a bifurcated hydrogen bond of  $C_3-H_3...N_1$  and  $C_5-H_5...N_1$ .

It is noteworthy that, the existence of two bifurcated hydrogen bonds for  $Al_{12}N_{12}$  and one for  $B_{12}N_{12}$  nanocage causes strong adsorption happened between the  $Al_{12}N_{12}$  and the octyl- $\beta$ -D-xyloside molecule. This factor can act as a negative force during the desorption of the octyl- $\beta$ -D-xyloside from the  $Al_{12}N_{12}$  nanocage and prolong the desorption time. The AIM analysis also represents the possibility of the formation of unconventional hydrogen bonds between the octyl- $\beta$ -D-xyloside and two nanocages. It is remarkably that the conventional hydrogen bond ( $O-H...N$ ) in all complexes is stronger than the unconventional ( $C-H...O$  and  $C-H...N$ ) due to the positive values of  $\nabla^2\rho(r)$  and negative value of  $H(r)$  which represents the medium hydrogen bond. Accordingly, in  $O_1-Al_{12}N_{12}$  complex; the conventional  $O_2-HO_2...N$  bond with  $\nabla^2\rho(r)=0.1142$  and  $H(r)=-0.0037$  is stronger than the unconventional  $C_8-H_8...O_5$  bond with  $\nabla^2\rho(r)=0.0346$ ,  $H(r)=0.0010$  and  $C_7-H_7...N$  with  $\nabla^2\rho(r)=0.0387$ ,  $H(r)=0.0011$ . In addition, the electron density of the  $O_n-Al$  bonds is almost half of the electron density of the  $O_n-B$  (i.e;  $\rho(r)=0.0508$  for  $O_3...Al$  but  $\rho(r)$

=0.0973 for O<sub>3</sub>...B). This is because the B<sub>12</sub>N<sub>12</sub> nanocage is smaller than the Al<sub>12</sub>N<sub>12</sub>, which makes the electron cloud more condense.

complex type (i): Form intra and intermolecular hydrogen bonding



Complex type (ii): Form intramolecular hydrogen bonding

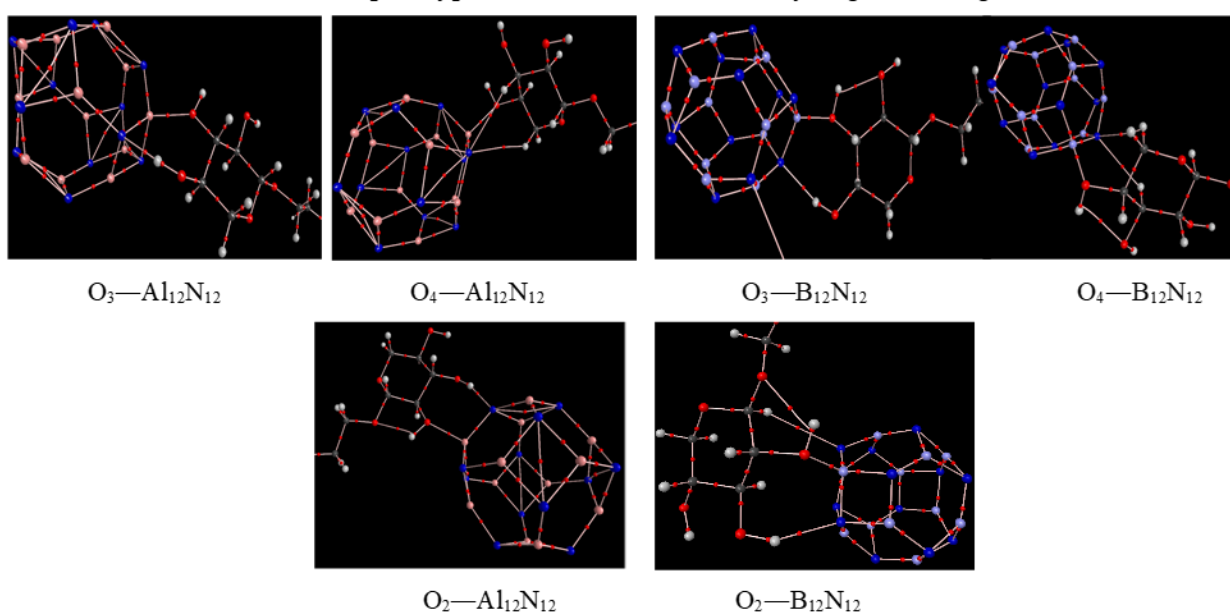


**Fig.7** The intra and intermolecular hydrogen bonding formation of different oxygen atoms of octyl- $\beta$ -D-xyloside over the Al<sub>12</sub>N<sub>12</sub> and B<sub>12</sub>N<sub>12</sub> nanocages at the B3LYP/6-311++G\*\* level of theory in the gas phase.

### 3.4 Conduction electron population

A gas sensor operates based on the change of its electrical conductivity upon the gas adsorption and charge transfer. It has been frequently demonstrated that the conduction electron population ( $N$ ), depends on the  $E_g$  based on Eq. (3) and can be applied as an appropriate index for an adsorbent sensitivity toward a chemical [37].

$$N = AT^{3/2}\exp\left(-\frac{E_g}{2KT}\right) \quad (3)$$

Where  $k$  is the Boltzmann's constant and  $A$  (electrons/m<sup>3</sup>K<sup>3/2</sup>) is a constant.

Equation 3 indicates that the population of conduction electrons of the Al<sub>12</sub>N<sub>12</sub> and B<sub>12</sub>N<sub>12</sub> nanocages will change exponentially by changing the  $E_g$  and will thus alter the electrical conductivity. From a conduction point of view, with the adsorption of the adsorbent, the change in conductivity is more desirable. Therefore, in this part, unlike the recovery time, which should be in a certain range, there is no such limitation for conduction change. This means that this quantity does not have to be in a certain range, and the larger it is for a sensor, the better [38]. The calculated conduction electron populations are given in Table 6. This factor shows the Al<sub>12</sub>N<sub>12</sub> and B<sub>12</sub>N<sub>12</sub> nanocages with high conduction electron population are suitable adsorbents for octyl- $\beta$ -D-xyloside in the gas phase. In both nanocages of Al<sub>12</sub>N<sub>12</sub> and B<sub>12</sub>N<sub>12</sub>, the O<sub>3</sub> position has the highest conduction electron population ( $N$ ). Therefore, the sensitivity of Al<sub>12</sub>N<sub>12</sub> and B<sub>12</sub>N<sub>12</sub> at the O<sub>3</sub> position is very good. The number of conducting electrons in Al<sub>12</sub>N<sub>12</sub> is larger than in B<sub>12</sub>N<sub>12</sub>. This fact demonstrates, from a conduction point of view, Al<sub>12</sub>N<sub>12</sub> behaves much better than B<sub>12</sub>N<sub>12</sub> to detect and absorb the octyl- $\beta$ -D-xyloside. In fact, based on the AIM results which showed the possibility of forming different bonds between the Al<sub>12</sub>N<sub>12</sub> and B<sub>12</sub>N<sub>12</sub> nanocages and the octyl- $\beta$ -D-xyloside molecule, we observed that Al<sub>12</sub>N<sub>12</sub> were more likely to adsorb octyl- $\beta$ -D-xyloside molecules with the possibility of forming two bifurcate bonds as well as the fewer possibility for intramolecular hydrogen bonds for octyl- $\beta$ -D-xyloside during the adsorption on the Al<sub>12</sub>N<sub>12</sub>.

**Table 6.** The calculated conduction electron population at the B3LYP/6-311++G\*\* level of theory in the gas phase.

Oxygen type	Complexes	$N(g)$
i: O <sub>1</sub> , O <sub>5</sub>	O <sub>1</sub> —Al <sub>12</sub> N <sub>12</sub>	$2.64 \times 10^{15}$
	O <sub>5</sub> —Al <sub>12</sub> N <sub>12</sub>	$7.94 \times 10^{13}$

ii: O <sub>3</sub> , O <sub>2</sub> , O <sub>4</sub> (hydroxyl groups)	O <sub>3</sub> —Al <sub>12</sub> N <sub>12</sub>	2.01 × 10 <sup>17</sup>
	O <sub>2</sub> —Al <sub>12</sub> N <sub>12</sub>	1.94 × 10 <sup>17</sup>
	O <sub>4</sub> —Al <sub>12</sub> N <sub>12</sub>	2.21 × 10 <sup>14</sup>
i: O <sub>5</sub> , O <sub>1</sub>	O <sub>5</sub> —B <sub>12</sub> N <sub>12</sub>	3.50 × 10 <sup>8</sup>
	O <sub>1</sub> —B <sub>12</sub> N <sub>12</sub>	1.51 × 10 <sup>8</sup>
ii: O <sub>3</sub> , O <sub>2</sub> , O <sub>4</sub> (hydroxyl groups)	O <sub>3</sub> —B <sub>12</sub> N <sub>12</sub>	8.04 × 10 <sup>10</sup>
	O <sub>2</sub> —B <sub>12</sub> N <sub>12</sub>	5.98 × 10 <sup>10</sup>
	O <sub>4</sub> —B <sub>12</sub> N <sub>12</sub>	2.44 × 10 <sup>9</sup>

### 3.5 Thermodynamic parameters

Table 8 represents the thermodynamic properties of the octyl- $\beta$ -D-xyloside adsorption through different oxygen atoms over the Al<sub>12</sub>N<sub>12</sub> and B<sub>12</sub>N<sub>12</sub> nanocages in the gas phase. According to Table 7, the O3 position in both nanocages has the lowest Gibbs free energy and enthalpies, which is in agreement with the adsorption energies from the O3 position. This can be related to the less spatial hinder around this position. On the other hand, the O1 and O5 positions have positive Gibbs free energy in B<sub>12</sub>N<sub>12</sub>. This is because, the unfavorable negative value of entropy overcomes the favorable negative of enthalpy and prevents the spontaneous adsorption from O1 and O5 positions. According to the thermodynamic parameters, the Al<sub>12</sub>N<sub>12</sub> is a promising candidate for the adsorption of molecule from O1, O2, O3, O4, and O5 positions, but the B<sub>12</sub>N<sub>12</sub> nanocluster shows spontaneous and favorable adsorption only from O2, O3, and O4 positions.

**Table 7.** The calculated thermodynamic properties; standard Gibbs free energy ( $\Delta G^\circ$ ), standard enthalpy ( $\Delta H^\circ$ ), and standard entropy ( $T\Delta S^\circ$ ), and all in (kJ.mol<sup>-1</sup>) for the studied complexes at the B3LYP/6-311++g\*\* level of theory with BSSE superposition error correction.

Oxygen type	Complex	$\Delta G^\circ$	$\Delta H^\circ$	$T\Delta S^\circ$
O1, O5	O <sub>1</sub> —Al <sub>12</sub> N <sub>12</sub>	-77.00	-126.52	-49.52
	O <sub>5</sub> —Al <sub>12</sub> N <sub>12</sub>	-63.57	-109.50	-45.93
O3, O2, O4	O <sub>3</sub> —Al <sub>12</sub> N <sub>12</sub>	-102.73	-148.42	-45.69

(hydroxyl groups)	O <sub>2</sub> —Al <sub>12</sub> N <sub>12</sub>	-102.27	-147.92	-45.65
	O <sub>4</sub> —Al <sub>12</sub> N <sub>12</sub>	-73.20	-114.16	-40.96
O <sub>5</sub> , O <sub>1</sub>	O <sub>5</sub> —B <sub>12</sub> N <sub>12</sub>	1.27	-49.10	-50.37
	O <sub>1</sub> —B <sub>12</sub> N <sub>12</sub>	7.03	-43.99	-51.02
O <sub>3</sub> , O <sub>2</sub> , O <sub>4</sub> (hydroxyl groups)	O <sub>3</sub> —B <sub>12</sub> N <sub>12</sub>	-26.13	-74.77	-48.64
	O <sub>2</sub> —B <sub>12</sub> N <sub>12</sub>	-23.70	-73.12	-49.42
	O <sub>4</sub> —B <sub>12</sub> N <sub>12</sub>	-13.22	-57.94	-44.72

### 3.6 Recovery time

Sensor recovery from the adsorbed gases is of great importance. The sensitivity and recovery time, are reported as the main performance parameters of a sensor. Recovery time is defined as the time required for a sensor to return to 90% of the original baseline signal upon removal of the target gas [36]. For a suitable sensor, the separation of the absorbed molecule is also very important. Experimentally the recovery process is done by heating to upper temperatures or by UV light exposure [34]. The recovery time can be calculated from transition theory:

$$\tau = \nu^{-1} \exp\left(\frac{-E_{ad}}{kT}\right) \quad (4)$$

where  $k$  is Boltzmann's constant ( $\sim 8.31 \times 10^{-3} \text{ kJ mol}^{-1} \cdot \text{K}^{-1}$ ),  $T$  is temperature, and  $\nu$  is the attempt frequency. Table 8 shows the recovery time of the investigated complexes. According to Eq.4, more adsorption energy leads to a larger recovery time. The order of the recovery time for desorption of octyl- $\beta$ -D-xyloside from Al<sub>12</sub>N<sub>12</sub> and B<sub>12</sub>N<sub>12</sub> nanocages for both types of oxygen atoms are; O<sub>3</sub> > O<sub>2</sub> > O<sub>4</sub>, O<sub>1</sub> > O<sub>5</sub> and O<sub>3</sub> > O<sub>2</sub> > O<sub>4</sub>, O<sub>5</sub> > O<sub>1</sub> respectively, which are in agreement with the order of the adsorption energies. Accordingly, O<sub>3</sub>—Al<sub>12</sub>N<sub>12</sub> and O<sub>3</sub>—B<sub>12</sub>N<sub>12</sub> complexes with the most adsorption energies have the maximum recovery time of  $5.11 \times 10^{10}$  and  $8.14 \times 10^{-3}$  s respectively. In terms of recovery time, Al<sub>12</sub>N<sub>12</sub> with a long recovery time may not be a good sensor for octyl- $\beta$ -D-xyloside, because octyl- $\beta$ -D-xyloside cannot detach itself in a reasonable time after attaching to Al<sub>12</sub>N<sub>12</sub>. On the other hand, there is a different scenario for B<sub>12</sub>N<sub>12</sub>. The recovery time for detaching octyl- $\beta$ -

D-xyloside from this nanocage is low. This means the octyl- $\beta$ -D-xyloside molecule can detach from the  $B_{12}N_{12}$  nanocage at a reasonable time. From this point of view,  $B_{12}N_{12}$  nanocage can behave as a good sensor for octyl- $\beta$ -D-xyloside. As a result, although all previously calculated parameters predicted better adsorption for octyl- $\beta$ -D-xyloside on the  $Al_{12}N_{12}$  than  $B_{12}N_{12}$ , a higher recovery time of  $Al_{12}N_{12}$  shows  $Al_{12}N_{12}$  can only use as a good adsorbent for octyl- $\beta$ -D-xyloside, not as a good sensor.

**Table 8.** The estimated recovery time ( $\tau$ ) in (s) for investigated complexes.

Oxygen type	Complexes	Gas.
i: O <sub>1</sub> , O <sub>5</sub>	O <sub>1</sub> —Al <sub>12</sub> N <sub>12</sub>	$8.80 \times 10^6$
	O <sub>5</sub> —Al <sub>12</sub> N <sub>12</sub>	$7.95 \times 10^3$
ii: O <sub>3</sub> , O <sub>2</sub> , O <sub>4</sub> (hydroxyl groups)	O <sub>3</sub> —Al <sub>12</sub> N <sub>12</sub>	$5.11 \times 10^{10}$
	O <sub>2</sub> —Al <sub>12</sub> N <sub>12</sub>	$4.75 \times 10^{10}$
	O <sub>4</sub> —Al <sub>12</sub> N <sub>12</sub>	$6.13 \times 10^4$
i: O <sub>5</sub> , O <sub>1</sub>	O <sub>5</sub> —B <sub>12</sub> N <sub>12</sub>	$1.54 \times 10^{-7}$
	O <sub>1</sub> —B <sub>12</sub> N <sub>12</sub>	$2.86 \times 10^{-8}$
ii: O <sub>3</sub> , O <sub>2</sub> , O <sub>4</sub> (hydroxyl groups)	O <sub>3</sub> —B <sub>12</sub> N <sub>12</sub>	$8.14 \times 10^{-3}$
	O <sub>2</sub> —B <sub>12</sub> N <sub>12</sub>	$4.50 \times 10^{-3}$
	O <sub>4</sub> —B <sub>12</sub> N <sub>12</sub>	$7.51 \times 10^{-6}$

## 4. Conclusion

The B3LYP/6-311++G\*\* method was employed to investigate the interaction between the octyl- $\beta$ -D-xyloside molecule from different oxygens with the  $Al_{12}N_{12}$  and  $B_{12}N_{12}$  nanocages in the gas phase. Based on the adsorption energies and enthalpies, a thermodynamically favorable chemisorption process was predicted for different complexes. The highest

adsorption energy was observed for the adsorption from O3 position of octyl- $\beta$ -D-xyloside molecule on both nanocages. The negative value of the Gibbs free energy of the O3 position in both nanocages confirmed the spontaneous adsorption process. The NBO analysis revealed in all complexes, the oxygen atoms of octyl- $\beta$ -D-xyloside molecule are electron-donating and the nanocluster is the electron acceptor. The estimated recovery time for adsorption on the  $\text{Al}_{12}\text{N}_{12}$  nanocage was very high which represents, against the high ability of  $\text{Al}_{12}\text{N}_{12}$  toward the adsorption of octyl- $\beta$ -D-xyloside, it cannot behave as a good sensor for the investigated molecule. The AIM results predicted the bifurcated hydrogen bonds for  $\text{Al}_{12}\text{N}_{12}$ , which can be good reason for high adsorption energies during the complexation with  $\text{Al}_{12}\text{N}_{12}$ . On the other hand, the recovery time for desorption from  $\text{B}_{12}\text{N}_{12}$  nanocage represented a possible desorption process. In summary, although the  $\text{Al}_{12}\text{N}_{12}$  and  $\text{B}_{12}\text{N}_{12}$  nanocages may be a promising candidate for detection of octyl- $\beta$ -D-xyloside molecule but the  $\text{Al}_{12}\text{N}_{12}$  with the high recovery time cannot used as a good sensor. It will be interesting to study the adsorption effect of decorated  $\text{B}_{12}\text{N}_{12}$  with metals with higher atomic number to improve its adsorption behavior along with its reasonable recovery time.

## References:

- [1] A. de Jesus Cortes-Sanchez, H. Hernández-Sánchez, M.E. Jaramillo-Flores, *Microbiol. Res.*, 168 (2013) 22-32.
- [2] L. Al-Araji, R.N.Z.R.A. Rahman, M. Basri, A.B. Salleh, *Asia-Pac. J. Mol. Biol. Biotechnol.*, 15 (2007) 99-105.
- [3] I.M. Banat, A. Franzetti, I. Gandolfi, G. Bestetti, M.G. Martinotti, L. Fracchia, T.J. Smyth, R. Marchant, *Appl. Microbiol. Biotechnol.*, 87 (2010) 427-444.
- [4] A. Zaragoza, F.J. Aranda, M.J. Espuny, J.A. Teruel, A. Marqués, A.n. Manresa, A. Ortiz, *Langmuir*, 25 (2009) 7892-7898.
- [5] D. Kitamoto, H. Isoda, T. Nakahara, *J. Biosci. Bioeng.* 94 (2002) 187-201.

- [6] L. Rodrigues, H.C. Van der Mei, J. Teixeira, R. Oliveira, *Appl. Environ. Microbiol.*, 70 (2004) 4408-4410.
- [7] S. Techaoei, *current applied science and technology*, 7 (2007) 230-238.
- [8] C.Y. Liew, M. Salim, N.I. Zahid, R. Hashim, *RSC Advances*, 5 (2015) 99125-99132.
- [9] D. Jimenes islas, S.A. Medina moreno, J.N. Gracida rodriguez, *Rev. Int. Contam. Ambient.*, 26 (2010) 65-84.
- [10] Q. Wang, Q. Sun, P. Jena, Y. Kawazoe, *ACS Nano* 3, 621 (2009).
- [11] S.G. Özkapı, B. Özkapı, H. Özkişi, S. Dalgıç, *Materials Today: Proceedings*, 4 (2017) 11644-11648.
- [12] K.-T. Yong, S.F. Yu, *J. Matls Sci*, 47 (2012) 5341-5360.
- [13] P. Weichi, L. Haiyang, Z. Xuejing, Z. Wenming, S. Ebrahimi, *Physics Lett A*, 384 (2020) 126396.
- [14] R. Nakanishi, R. Kitaura, J.H. Warner, Y. Yamamoto, S. Arai, Y. Miyata, H. Shinohara, *Scientific reports*, 3 (2013) 1-6.
- [15] Y. Wei, P. Liu, *Strucl Chem*, (2021) 1-8.
- [16] S. Munsif, K. Ayub, *J. Mol. Liq*, 259 (2018) 249-259.
- [17] K. Narsaiah, S.N. Jha, R. Bhardwaj, R. Sharma, R. Kumar, *J. food sci and tech*, 49 (2012) 383-406.
- [18] T.P.I.C. Del tittoto, D.R. Di Dottore, *Synthesis and bio-functionalization of nanoparticles for biosensing and biorecognition. J. Mol. Liq*, 176 (2020) 310-321.
- [19] E. Rauls, S. Blankenburg, W. Schmidt, *Surface sci*, 602 (2008) 2170-2174.
- [20] A.S. Rad, K. Ayub, *J. Alloys Comds*, 672 (2016) 161-169.
- [21] S. Sagadevan, M. Periasamy, *Rev. Adv. Mater. Sci.*, 36 (2014).
- [22] J. Beheshtian, M. Kamfiroozi, Z. Bagheri, A. Ahmadi, *Comput. Mater. Sci*, 54 (2012) 115-118.

- [23] G. Seifert, P. Fowler, D. Mitchell, D. Porezag, T. Frauenheim, *Chem Phys Lett*, 268 (1997) 352-358.
- [24] Y. Yong, K. Liu, B. Song, P. He, P. Wang, H. Li, *Physics Letters A*, 376 (2012) 1465-1467.
- [25] S. Javarsineh, E. Vessally, A. Bekhradnia, A. Hosseinian, S. Ahmadi, *J. Cluster Sci*, 29 (2018) 767-775.
- [26] M.T. Baei, M.R. Taghartapeh, E.T. Lemeski, A. Soltani, *Physica B: Condensed Matter*, 444 (2014) 6-13.
- [27] J. Beheshtian, A.A. Peyghan, Z. Bagheri, *Computational matls sci*, 62 (2012) 71-74.
- [28] S.F. Boys, F. Bernardi, *Molelar Phys*, 19 (1970) 553-566.
- [29] A. Shokuhi Rad, K. Ayub, *J Alloys Compd*, 672 (2016) 161-169.
- [30] R. Bader, *Atoms in molecules. A quantum theory*, Oxford University Press, Oxford, 1995.
- [31] P. Popelier, *J Phys Chem A*, 102 (1998) 1873-1878.
- [32] W. Saenger, G. Jeffrey, *Hydrogen bonding in biological structures*, in, Springer-Verlag, Berlin, 1991.
- [33] G.A. Jeffrey, *An introduction to hydrogen bonding*. Oxford university press, New York 1997.
- [34] Z.M. Kotena, A. Fattahi, *J Mol Graph Model*, 98 (2020) 107612.
- [35] Z.M. Kotena, S.B. Mohamad, *B.Mol Cryst Liq Cryst*, 646 (2017) 31-40.
- [36] C.H. Görbitz, M.C. Etter, *J Chem Soc, Perkin Transactions 2*, (1992) 131-135.
- [37] S.J. Grabowski, *Hydrogen bonding: new insights*, Springer, Netherlands, 2006.
- [38] N. Nepal, K. Nam, J. Li, M. Nakarmi, J. Lin, H. Jiang, *Appld phys lett*, 88 (2006) 261919.